SSRG International Journal of Electrical and Electronics Engineering
ISSN: 2348-8379/ https://doi.org/10.14445/23488379/IJEEE-V11I5P130

Volume 11 Issue 5, 323-335, May 2024

Original Article

Integrated Photovoltaic Energy System with High-Gain Multiport DC-DC Converter and Modified ANFIS Control for Robust DC Power Supply

Sundar Ramakrishnan[1], Porkumaran Karantharaj[2]

[1]*Department of Biomedical Engineering, Dr. N.G.P. Institute of Technology, Tamil Nadu, India.*
[2]*Sri Sairam Engineering College, Tamilnadu, India.*

[1]*Corresponding Author : sundarcute88@gmail.com*

Received: 19 March 2024 Revised: 18 April 2024 Accepted: 15 May 2024 Published: 29 May 2024

Abstract *- Renewable Energy Resources (RES) have become integral components of energy strategies worldwide, witnessing a widespread adoption across various applications. The prevalent utilization of these resources can be attributed to their efficiency, cost-effectiveness and the growing global demand for energy. As daily energy consumption continues to rise, the popularity of renewable energy resources persists, driven by their effectiveness and economic viability across diverse sectors. The proposed system constitutes a Photovoltaic (PV) energy generation system integrated with a high-gain multi-port DC-DC converter, ultimately powering a DC load. The high-gain multi-port DC-DC converter serves as a pivotal component, efficiently managing power flow between the PV source and the DC load. Notably, the DC link voltage, critical for sustained operation, is adeptly regulated by a Modified Adaptive Neuro-Fuzzy Inference System (ANFIS) controller. This controller optimally adjusts the converter's operation, ensuring the stability and reliability of the entire system. The significance lies in the synergy between renewable energy harvesting through PV panels, the versatile multi-port converter and the intelligent control facilitated by the Modified ANFIS, collectively fostering an energy-efficient and robust DC-based power system. The battery system is employed to store surplus energy attained from the PV system, which can be utilized in the lagging period of energy. The overall proposed system is implemented in MATLAB/Simulink. This comprehensive approach not only harnesses solar energy effectively but also showcases the adaptability and precision achieved through advanced control strategies, making it a promising model for sustainable energy applications.*

Keywords *- High gain multi-port converter, MATLAB/Simulink, Modified ANFIS, Photovoltaic, RES.*

1. Introduction

Due to the growing number of people, businesses and residents worldwide, there is an urgent need for electricity. In the past, fossil fuels were used to generate electricity; however, the use of fossil fuels has historically exacerbated environmental issues and disrupted the global ecosystem [1, 2]. Nuclear energy and renewable energy sources are essential substitutes for fossil fuels in order to solve this issue [3].

Today's renewable energy sources are low-polluting and sustainable, among their numerous benefits. These days, one of the RES, known as solar photovoltaic generation, is becoming a more appealing option to traditional energy sources fossil fuels because of its lower energy costs, flexibility in terms of scale, and ease of procurement, low maintenance requirements and pollution-free operation [4, 5]. However, the environment, including temperature, solar light and shifting shadows, has a significant impact on the amount of energy generated by highly erratic and intermittent SPV systems [6]. Traditionally, a pre-conditioning DC/DC converter is needed for the renewable power generating system in order to improve isolation, maintain a steady power output, and achieve full energy harvesting [7]. Researchers and engineers have been attempting to create sophisticated power electronics converters and PV system control schemes in order to overcome these obstacles [8].

A DC-DC boost converter is essential to raise the low voltage to the required level when the voltage across renewable energy sources is low, making grid integration unfeasible [9]. The issue with DC-DC boost converters is that they must run at high-duty cycles in order to increase voltage. This imposes much strain on the power semiconductor devices they use, which reduces overall efficiency and limits voltage gain [10, 11]. One such solution is the high-gain multi-port DC-DC converter, which enables efficient power transfer between multiple ports, such as the PV array, energy storage devices and loads. This converter offers several advantages,

including high conversion efficiency, compact size, and flexibility in managing power flow.

In addition to the converter, control algorithms play a vital role in optimizing the performance of PV systems [12, 13]. In this context, conventional techniques like Fuzzy [14, 15], Artificial Neural Networks (ANN) [16] and ANFIS control technique [17] have gained popularity. ANFIS combines the advantages of neural networks and fuzzy logic to create a robust and adaptive control system. By utilizing ANFIS, the control strategy can effectively regulate the voltage and current levels and ensure a reliable and stable DC power supply [18, 19]. Due to issues including the curse of dimensionality and computational cost, ANFIS is not suitable for solving problems involving huge input sizes [20, 21]. As a consequence, the proposed work implemented the Modified ANFIS controller to overcome the issues in the normal ANFIS controller, which led to improved accuracy, reduced control errors and better overall control performance.

Furthermore, the PV systems generate electricity from sunlight during the day, but the energy production is intermittent and dependent on weather conditions. Batteries allow for the storage of excess energy generated during sunny periods for later use when sunlight is not available, such as during the night or on cloudy days. Energy storage helps ensure a continuous and reliable power supply, making the PV system more self-sufficient and reducing reliance on the grid.

The contributions of the developed work are illustrated as follows,

- High-gain multi-port DC-DC converter is employed to efficiently manage the power flow between the PV source and the DC load.
- The Modified ANFIS controller is employed to adjust the converter's operation optimally, ensuring the stability and reliability of the entire system.
- The battery system is utilized to store the surplus energy obtained from the PV system, which distributes the power supply to the load system during the lagging period of energy from PV.

2. Proposed Methodology

The integration of PV energy systems into power infrastructure has gained significant attention due to the increasing demand for RES and the need to reduce greenhouse gas emissions. PV systems harness the power of sunlight and convert it into electrical energy, providing a clean and sustainable power generation solution.

To ensure the efficient utilization of the generated PV power, converter and control techniques are employed. One such advanced solution is the integration of a high-gain multi-port DC-DC converter and a Modified ANFIS control for a robust DC power supply. The Flow diagram of the proposed work is illustrated in Figure 1, and it is explained as follows,

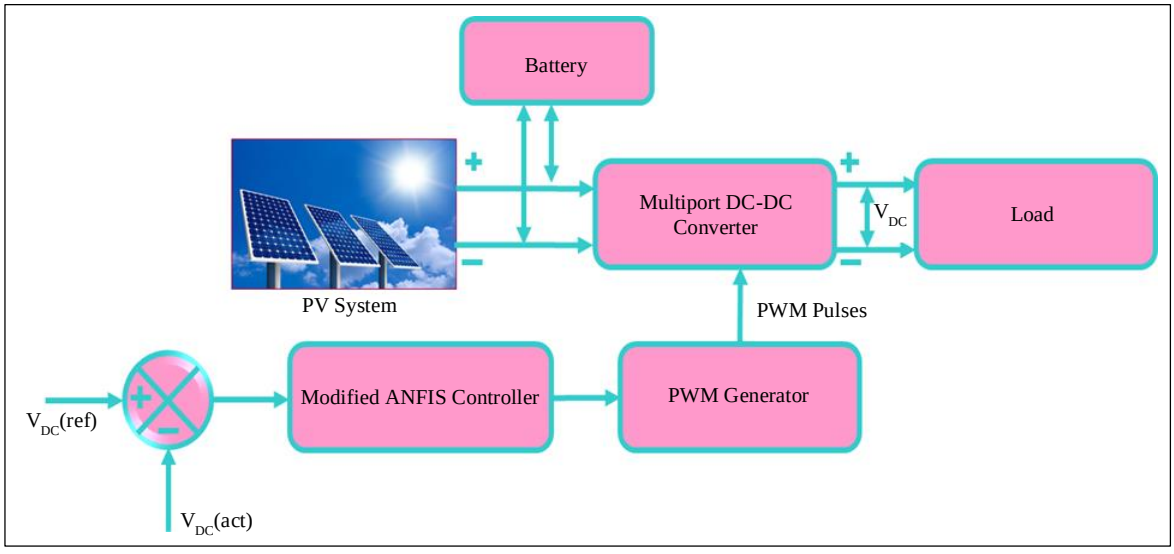

Fig. 1 Block diagram for the proposed framework

The low output voltage from the PV system is delivered to the Multi-port DC-DC converter, which efficiently manages the power flow from the PV panels. This ensures maximum energy harvesting capability and increases the overall efficiency of the system. The reference voltage is compared with the actual voltage that generates the error signal; for compensating this the Modified ANFIS controller is implemented. This helps to maintain a stable and reliable power output, even in the presence of changing environmental conditions or varying load demands. The controlled output is fed to the PWM generator for producing pulses for the better working of the proposed converter. On the other hand, the

battery system is employed to store surplus power from the PV system. During the lagging period of energy from the PV system due to ecological changes, the battery system generates power for the load application. Finally, the proposed system's robustness ensures a consistent and reliable DC power supply, which is essential for various applications and loads.

2.1. Modelling of PV System

In general, a solar cell consists of a power source coupled in parallel with an inverted diode. It represents parallel connections with series resistors and series connections with parallel resistors, respectively. Leakage currents result in parallel resistance, whereas a disturbance in the direction of electron migration from n to p junction creates series resistance. The equation that follows represents the PV current at the output end,

$$I = I_{SCC} - I_d \tag{1}$$

$$I_d = I_O\left(e^{\frac{qVd}{KT}} - 1\right) \tag{2}$$

Here, I_d specifies the current over the diode, I_O indicates the reciprocal of diode current saturation, q represents the electron of charge, I_{SCC} denotes the current of the short circuit in the PV panel and V_d refer to the voltage over the diode respectively. By resolving Equation (1) and (2),

$$I = I_{SCC} - I_O\left(e^{\frac{qVd}{KT}} - 1\right) \tag{3}$$

Here, I stands for PV cell current, V for PV cell voltage, and n for the diode ideality factor.

2.2. Modelling of DC-DC Multiport Converter

The proposed step-up converter with three input ports for a hybrid energy system is shown in Figure 3. The power semiconductor switches s_1, $s_2$and s_3 regulate the three input sources.

Diodes were used to freewheel the current when the power semiconductor switch was in the OFF state, and inductors and capacitors served as converter filtering components. The steady-state output voltage across the load "R" of the three-input port step-up converter is supplied by,

$$V_O = \sum_{J=1}^{3} \frac{V_j}{1-d_j} \tag{4}$$

Here, the power semiconductor switch s_1, s_2 operating duty cycle is shown by d_j, and the three-input step-up converter output voltage is represented by V_O. For switches s_1, s_2 the gating signal is shown in Figure 5. Figure 4 illustrates how the converter functions in various modes, including modes 1, 2, and 3.

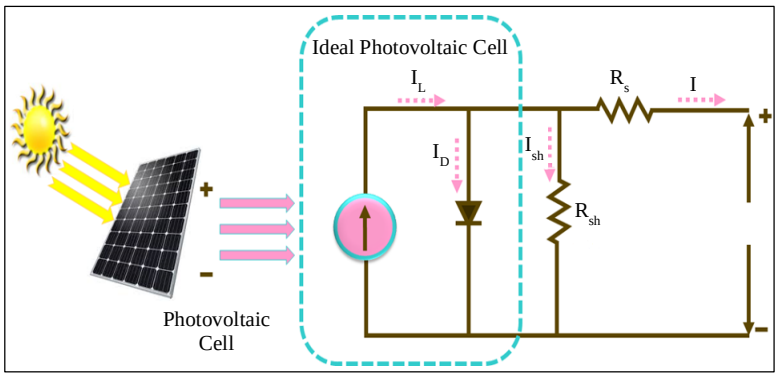

Fig. 2 Structure of solar PV system

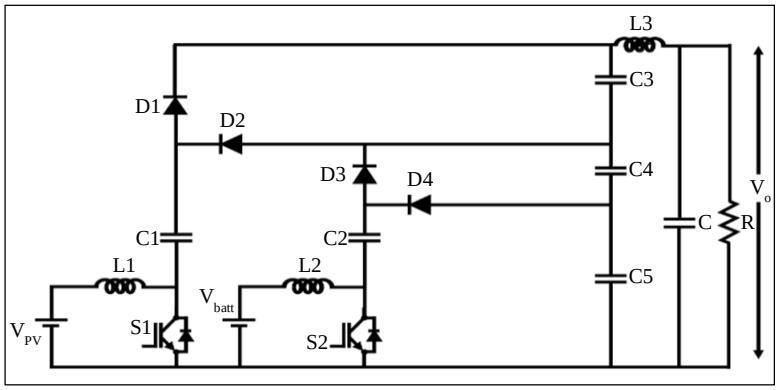

Fig. 3 Circuit diagram of proposed multi-port DC-DC converter

Mode 1: In this state, power switches s_1, s_2 are activated as specified in Figure 4(a). The currents of the inductors L_1, L_2 increase linearly as a result of the input voltages. All of the diodes are reversely biased and do not conduct, so the voltage of the capacitors stays constant. In this mode 1, the output capacitor supplies the output load.

Mode 2: This mode, s_1 is in ON state and s_2 in the OFF state, Diodes D_1 and D_3 are reverse-biased, while diodes D_2, D_4 are forward-biased. The capacitors C_2, C_4 are charged while capacitors C_1, C_3 and C_5 are discharged in this mode. The output capacitor C provides power to the load.

Mode 3: In this mode, the Power switches s_1 and s_2 are in OFF condition. Forward-biased diodes are D_1 and D_3 While reverse-biased diodes are D_2, D_4. The odd-numbered capacitors C_1, C_3 and C_5 are charged by the current passing through the primary and secondary inductors L_1 and L_2, and the even-numbered capacitors C_2, C_4 are discharged. The inductor L_3 provides power to the load and output capacitors.

The inductors' average current can be written as

$$iL1_{avg} = \frac{M}{1-d_1} I_{out} \quad (5)$$

$$iL2_{avg} = \frac{M}{1-d_2} I_{out} \quad (6)$$

$$iL3_{avg} = \frac{M}{1-d_3} I_{out} \quad (7)$$

Here, M specifies the voltage gain of the developed converter and I_{out} indicates average output current respectively.

Three-input step-up converters have boost cell inductors that are constructed similarly to those of conventional boost converters. The converter's Continuous Conduction Mode is intended to operate with inductors (CCM). The following formula can be used to determine the minimum rate of inductors for the CCM converter process:

$$L_{1min} = \frac{(1-d_1)d_1 V_{pv}}{2MI_{out}f_{sw}} \quad (8)$$

$$L_{2min} = \frac{(1-d_2)d_2 V_{batt}}{2MI_{out}f_{sw}} \quad (9)$$

$$L_{3min} = \frac{(1-d_3)d_3 V_o}{2MI_{out}f_{sw}} \quad (10)$$

Here, V_{pv}, V_{batt} represents the input voltage PV and battery, f_{sw} indicates the switching frequency of the converter. For step-up converters with three inputs, the capacitor value is as follows:

$$C_{1,min} = C_{1,min} = C_{1,min} = \frac{\lambda V_o}{f_{sw} R_{Lmin} V_{PP,max}} \quad (11)$$

Here, $V_{PP,max}$ indicates the maximum ripple voltage and the R_{Lmin} represents the converter's minimum load resistance correspondingly.

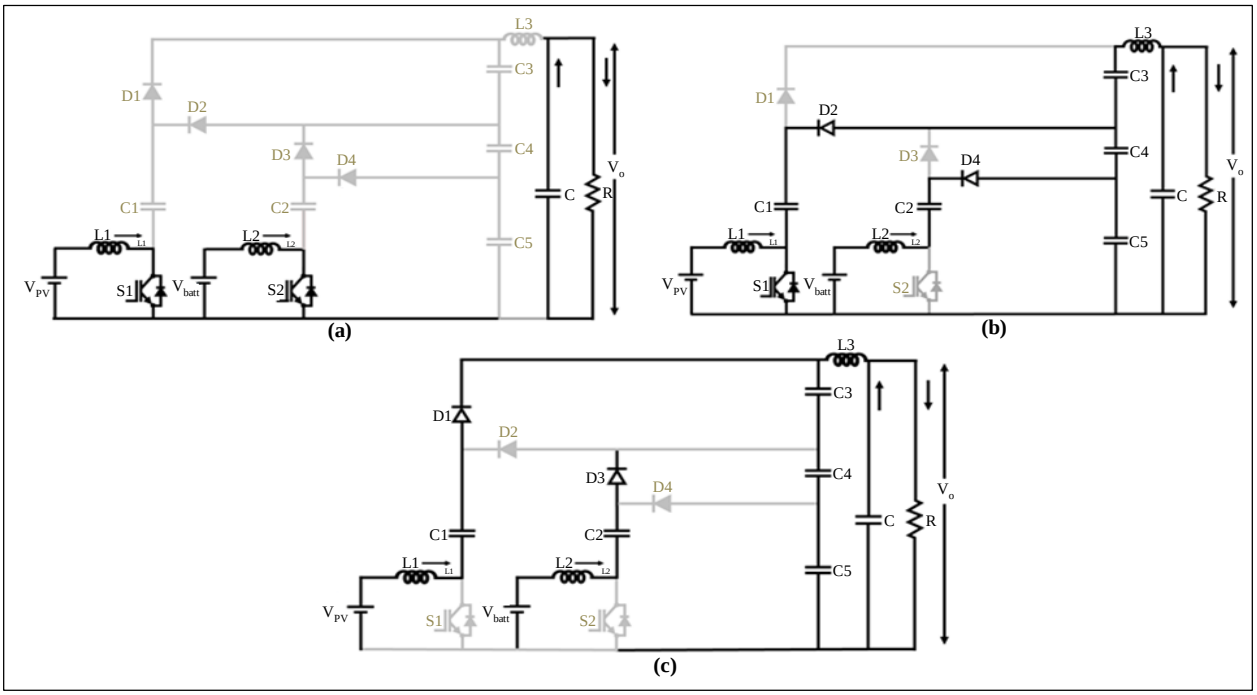

Fig. 4 Modes of operation (a) Mode 1, (b) Mode, and (c) Mode 3.

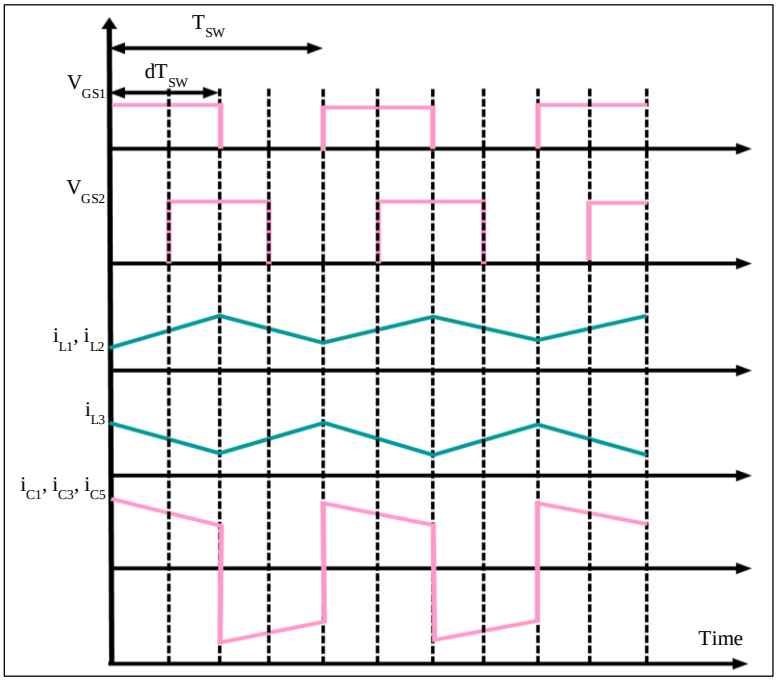

Fig. 5 Waveform for the proposed converter

2.3. Modelling of Modified ANFIS Controller

One of the problems with using a traditional fuzzy technique is the correlation between computing difficulty and ANFIS dimensions, which is also known as the "curse of dimensionality." In order to break the curse, it definitely needs to reevaluate the Modified ANFIS (MANFIS) architecture seen in Figure 6.

Four layers make up a standard ANFIS model; the defuzzification layer is the fourth layer; in this layer, every rule will produce a distinct output. The normalized emission intensity multiplied by the first-order polynomial function yields the output for each adaptive node in this layer:

$$O^4{}_i = \bar{w}_i f_i = \bar{w}_i(p_i x + q_i y + r_i). \quad i = 1,2 \qquad (12)$$

In formula (13), the posterior parameter set is denoted by $\{p_i, q_i, r_i\}$, and $\bar{w}_i$ indicates the output of the third layer of the ANFIS structure. In Formula (13), the Taylor series is extended as follows:

$$f_i \approx f_i(c^i) + \frac{df_i}{dx^i{}_1}(x^i{}_1 - c^i{}_1) + \cdots + \frac{df_i}{dx^i{}_n}(x^i{}_n - c^i{}_n) \qquad (13)$$

Where $\frac{df_i}{dx^i{}_n}$ specifies the function gradient of the ith rule centre, $f_i(c^i)$ represents the basic function value of the ith rule centre, and n is the input dimension. The rule centre, which has the same dimension as the input, is represented by the formula $c^i = [c^i{}_1, x^i{}_n]$. As a result, the ANFIS first-order model can be written as:

$$f_i \approx \sum_{i=1}^{R}(f_i(c^i) + \sum_{n=1}^{N}(x^i{}_n - c^i{}_n)).\bar{w}_i \qquad (14)$$

Using the zero-order ANFIS model, fi(c i) can be found in this formula. Domain expertise is combined into the model as a Gauss basis function in the manner shown below:

$$\Phi^j{}_r = a^j.exp\left(-\sum_{i=1}^{n}\left(\frac{c^B{}_i - c^F{}_i}{\sigma^j{}_i}\right)^2\right) \qquad (15)$$

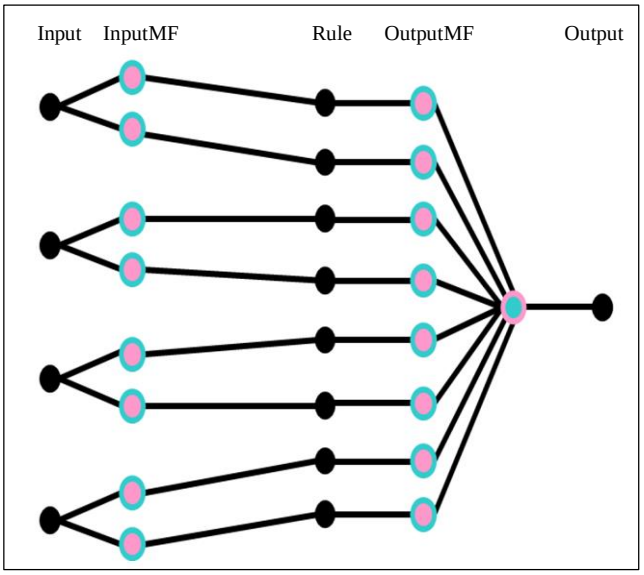

Fig. 6 Structure of modified ANFIS

This is the favorable rule of Set R and is composed of the elements $j \in J$, $r \in R$ and $\in R$. $(c^B{}_1, c^B{}_2, c^B{}_i, c^B{}_n)$ And $(c^F{}_i = c^F{}_1, c^F{}_2, c^F{}_i, c^F{}_n)$are the centers of rth and jth rules that are presented in sets B and F, respectively. B And F are two distinct data sets. To simulate domain knowledge, the

Gauss basis function is employed. When there are many advantageous rules, the weighted geometric mean of the independent Gauss function can be used to represent the model's output in the rth rule.

$$m^r{}_o = \prod_{j=1}^{J} (\Phi^j{}_r)^{\gamma_r{}^j} \quad (16)$$

$$\gamma_r{}^j = \frac{1}{\Sigma_{i=1}^{J} \left({}^{D_{rj}}/_{D_{ri}} \right)} \quad (17)$$

Where the parameter generated by the zero-order ANFIS model's rth rule is denoted by $m^r{}_o$. The weight of the degree between the jth suitable rule centers and the rth rule centers is represented by $\gamma_r{}^j$ respectively.

3. Results and Discussion

The proposed system constitutes a PV energy generation system integrated with a high-gain multi-port DC-DC converter, ultimately powering a DC load. The proposed High gain converter efficiently manages the power flow between the PV source as well as the DC load.

On the other hand, the Modified ANFIS controller effectually controlled the developed converter with less settling time. By utilizing MATLAB/Simulink, the proposed work is validated, and the comparative analysis is made, which is designated in this section. Table 1 specifies the parameter specification, which is discussed as follows.

Table 1. Parameter specification

Parameters	Values
Number of Cells Connected in Series N_s	36
Peak Power	10KW, 10 Panels
Open Circuit Voltage	12V
Short Circuit Current	8.3A
High-Gain Multi-Port Converter	
Switching Frequency	10KHz
L_1, L_2, L_3	1mH
C_1, C_2, C_3, C_4, C_5	22µF
C_o	2000µF

3.1. Case 1 Single Input Single Output (SISO)

The PV waveform gets medium Temperature and Irradiation of 35 °C and 1000(w/sq.m) correspondingly as specified in Figure 7(a) and (b). As illustrated in Figure 7 (b) and (c), the solar panel input voltage is taken as 76V and the current is 13.1A, respectively.

As indicated in Figure 8 (a) and (b), the output current oscillates certain period, and it is constantly maintained at 400V, and the output current is also upheld initially after it is preserved at 2.31A. Furthermore, the input power is given as 1000W, and the output power is preserved at 922W, as specified in Figure 8 (c) and (d). In this case 1, the battery is unable to charge due to insufficient power.

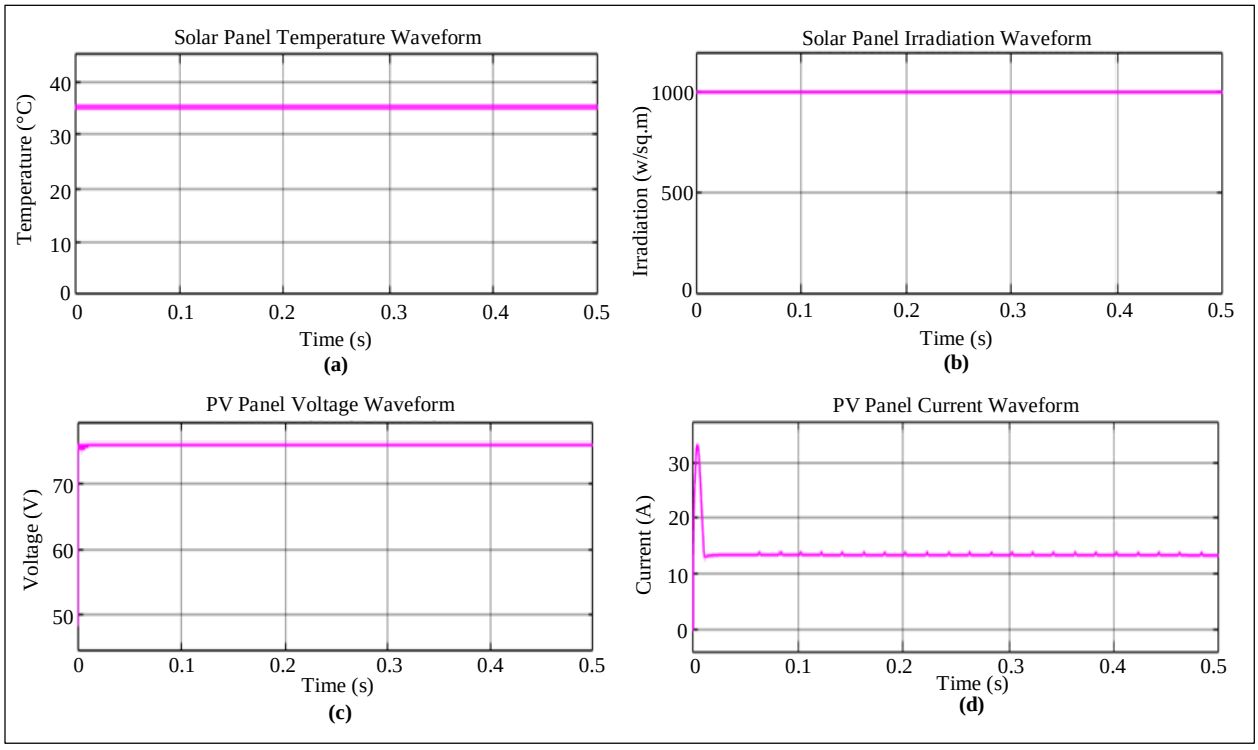

Fig. 7 Solar panel waveform (a) Temperature, (b) Irradiation, (c) Voltage, and (d) Current.

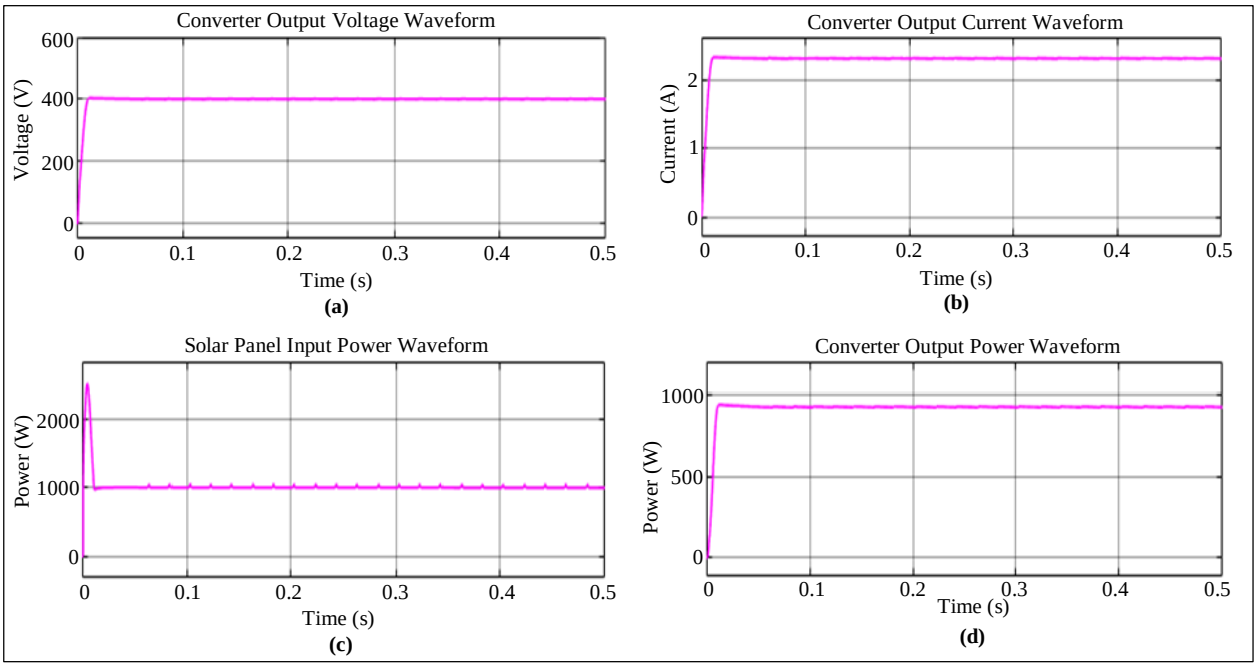

Fig. 8 Waveforms (a) Converter output voltage, (b) Output current, (c) Solar panel input power, and (d) Converter output power.

3.2. Case 2 Double Input Single Output (DISO)

In this case, the solar panel gets low temperature and radiation of 20°C and 700(w/sq.m), as demonstrated in Figure 9(a) and (b). Moreover, the voltage and current obtained from the PV are 58V and 11.97A, respectively. The power attained from the PV is 700W, which is lower than the load power of 1000W, as specified in Figure 10(a). The battery voltage gets preserved at 50V and the current is unity as illustrated in Figure 10 (b) and (c) respectively.

Figures 11(a), and (b) illustrate the converter output voltage and current waveform, which is observed that the output voltage gets constantly preserved at 400V. Similarly, the current oscillates for a certain period, and it is constantly upheld at 3A. Furthermore, the battery power initially oscillated after 0.1s, it is constantly preserved at 300W, and the converter output power is constantly maintained at 922W, as illustrated in Figure 12(a) and (b). Thus, the battery needs to distribute the load demand of 300W.

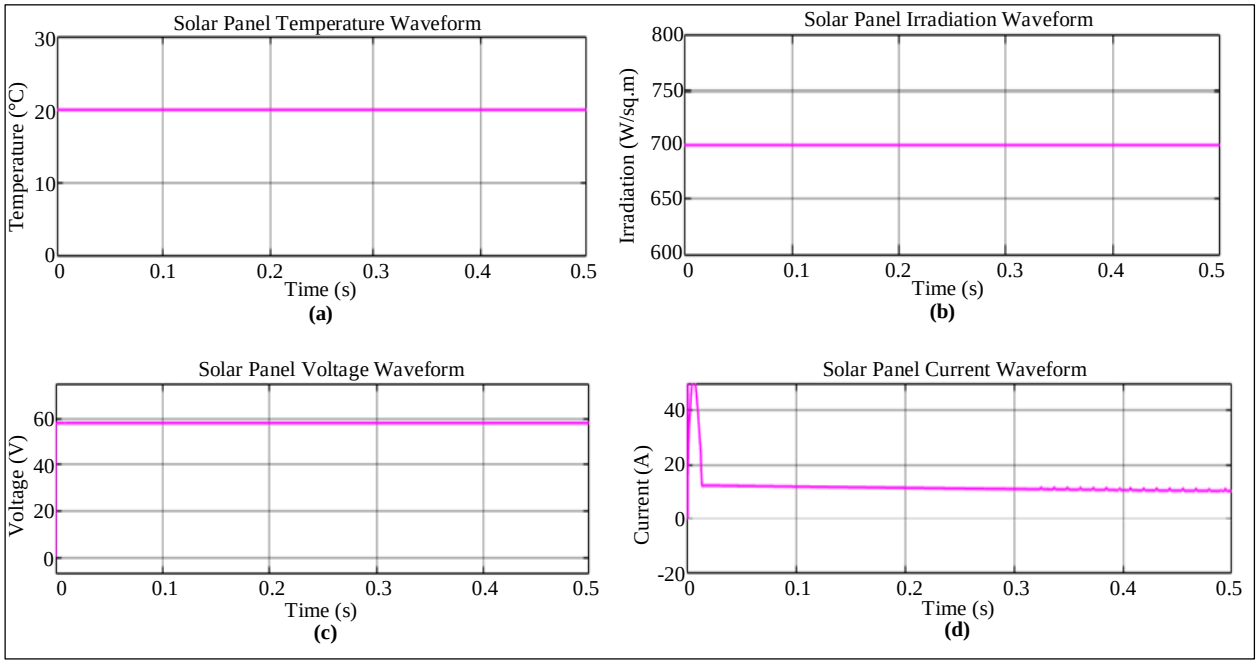

Fig. 9 Solar panel waveform (a) Temperature (b) Irradiation (c) Voltage, and (d) Current.

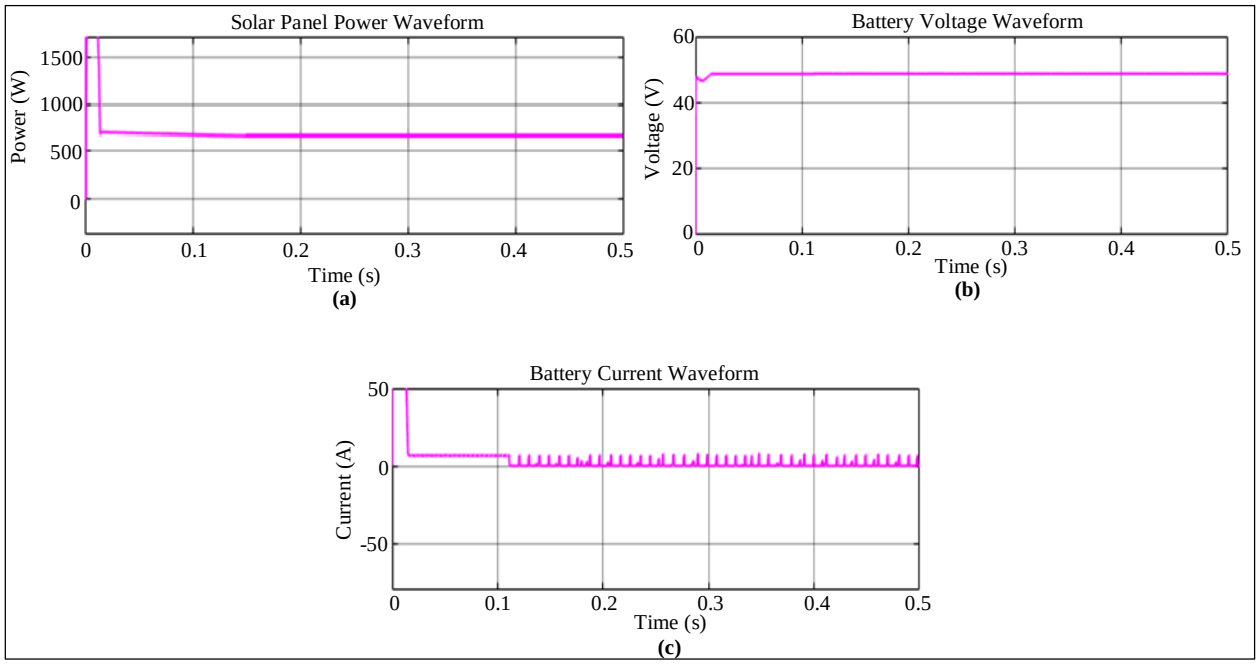

Fig. 10 (a) Solar panel power, (b) Battery voltage, and (c) Battery current waveform.

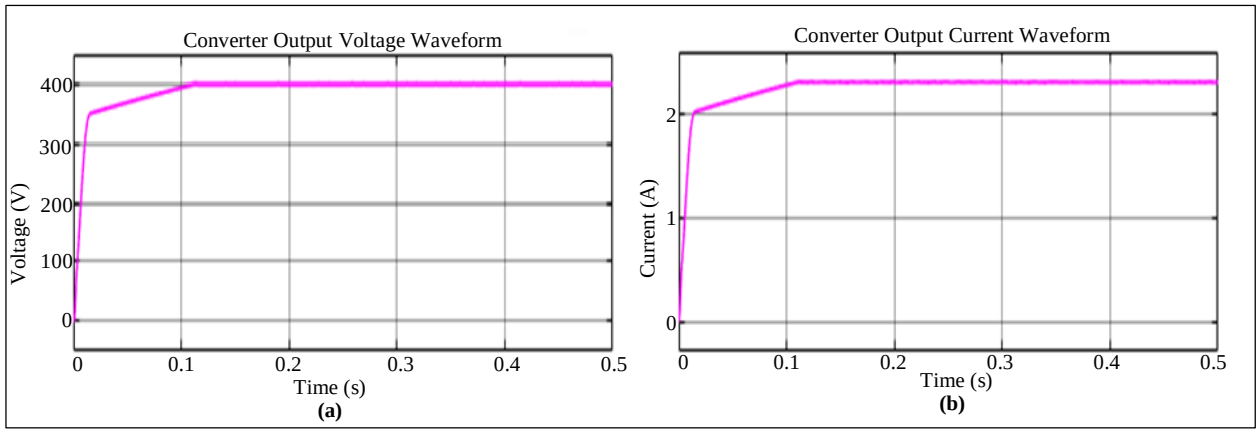

Fig. 11 Converter output (a) Voltage, and (b) Current waveform.

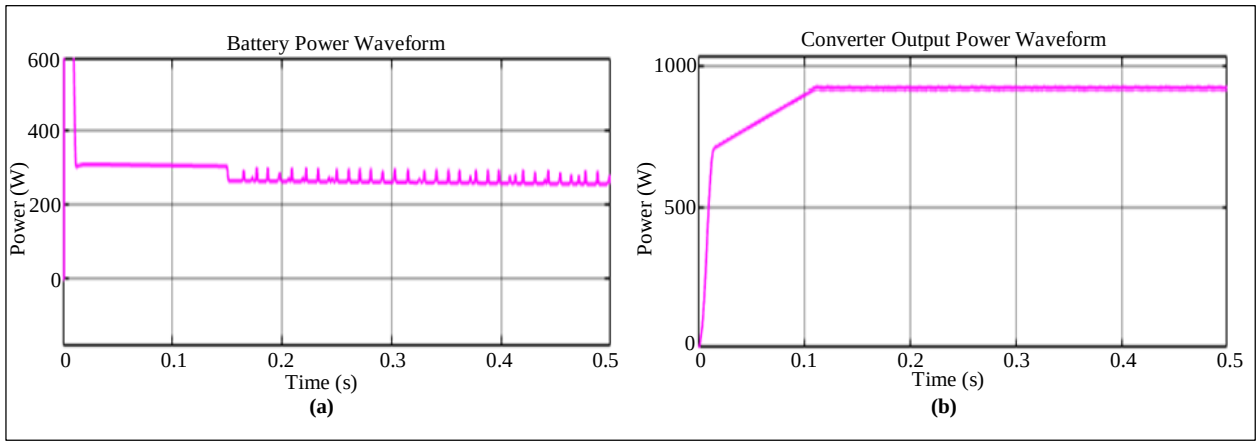

Fig. 12 Output power waveform (a) Battery, and (b) Converter.

3.3. Case 3 Single Input Double Output (SIDO)

As specified in Figure 13 (a) and (b), the PV panel gets maximum irradiation and temperature of 35°C and 1000(w/sq.m) in this case. Furthermore, as specified in Figures 13 (c) and (d), the PV panel obtained voltage and current are 76V and 10.9A, correspondingly. Similarly, the converter output voltage is constantly preserved at 400V, and the current is maintained at 1.8A after fluctuating a certain time, as indicated in Figure 14 (a) and (b). The solar power input is 817W, and the output power of the converter is maintained at 755W after fluctuating a certain time, as illustrated in Figure 14 (c) and (d).

The battery waveform is demonstrated in Figure 15, which shows that the battery voltage is constantly preserved at 50V, and the current is maintained at -2A. Moreover, the battery power is constantly upheld at -183W because, during battery charging, the current gets a negative value. The converter output voltage waveform using various controllers is illustrated in Figure 16; from the result, it is analyzed that using the PI controller, the voltage gets oscillated certain period, and after 0.2s, it constantly upheld at 400V and by utilizing the ANFIS controller, the voltage is maintained after 0.12s. Similarly, the proposed Modified ANFIS controller has constantly maintained its voltage at 400V after 0.02s.

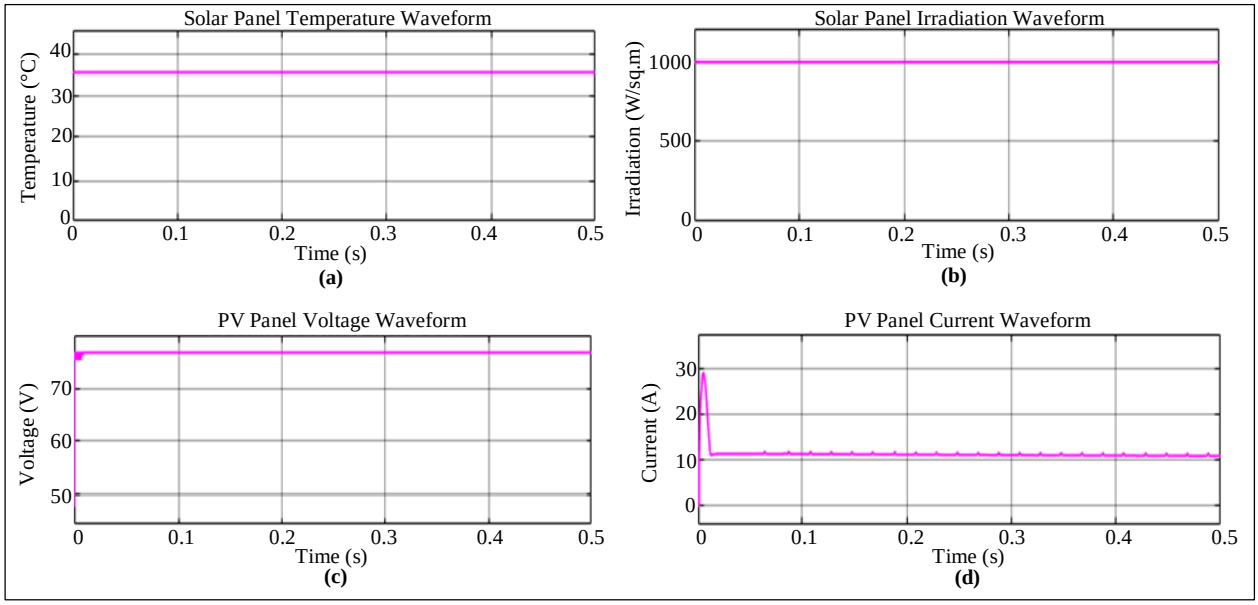

Fig. 13 Solar panel waveform (a) Temperature, (b) Irradiation, (c) Voltage, and (d) Current.

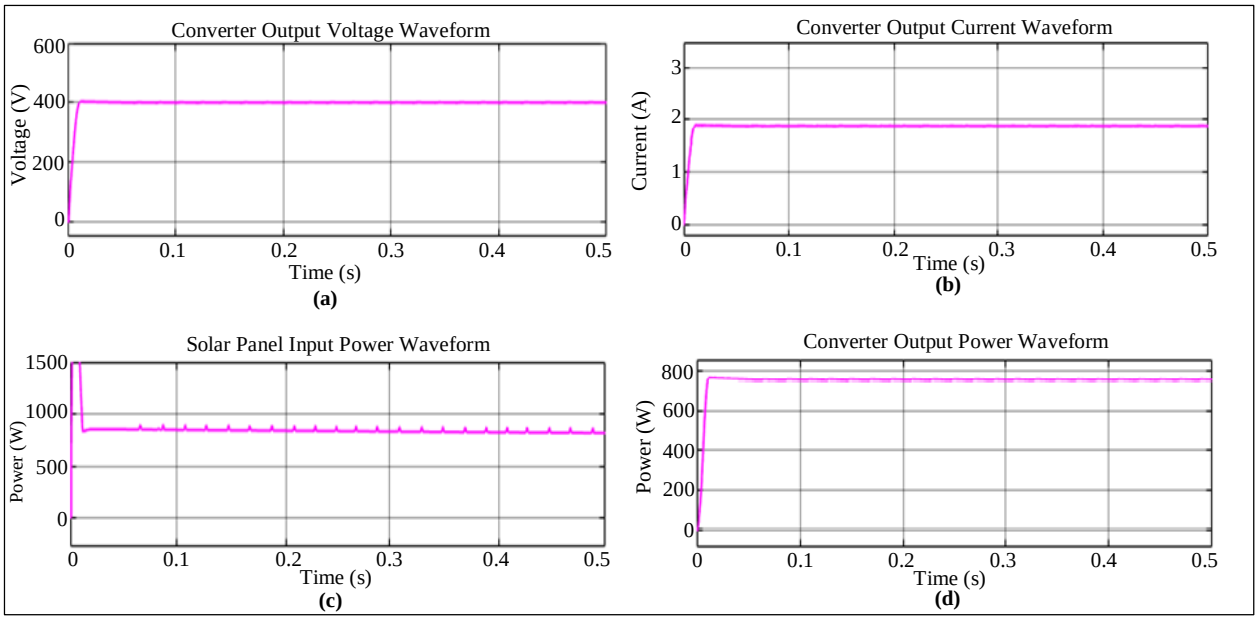

Fig. 14 Waveforms (a) Converter output voltage, (b) Converter Output current, (c) Solar panel input power, and (d) Converter output power.

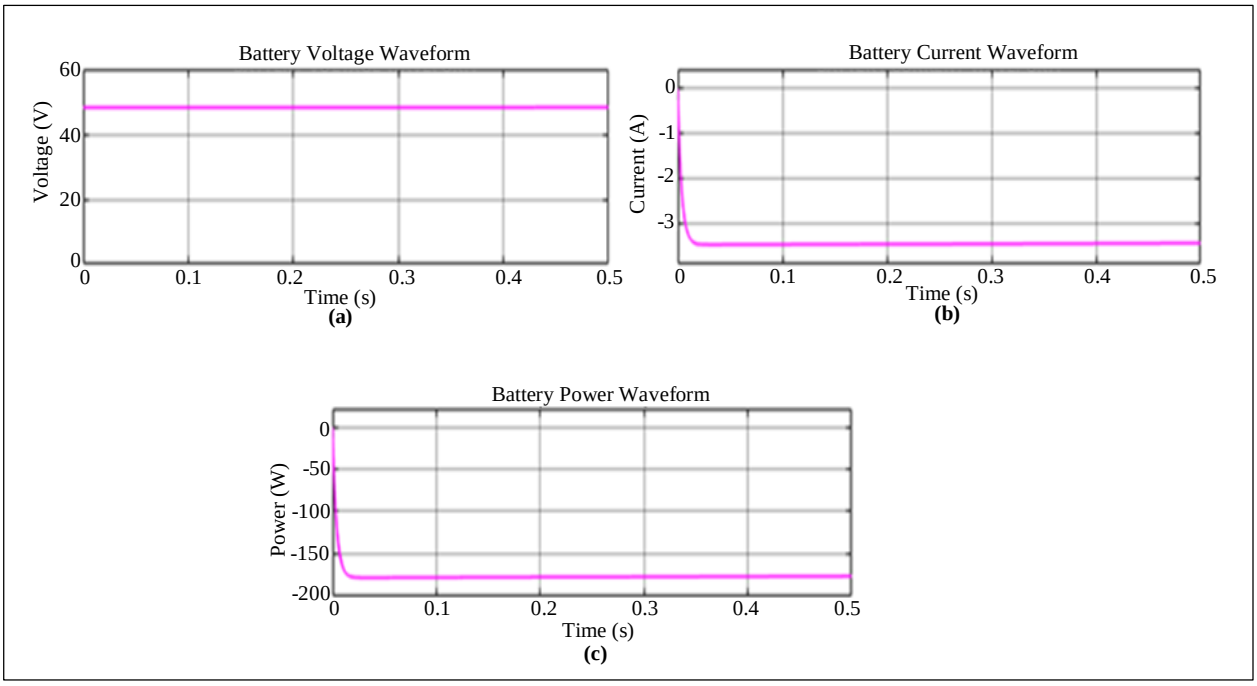

Fig. 15 (a) Battery voltage, (b) Current waveform, and (c) Power waveform.

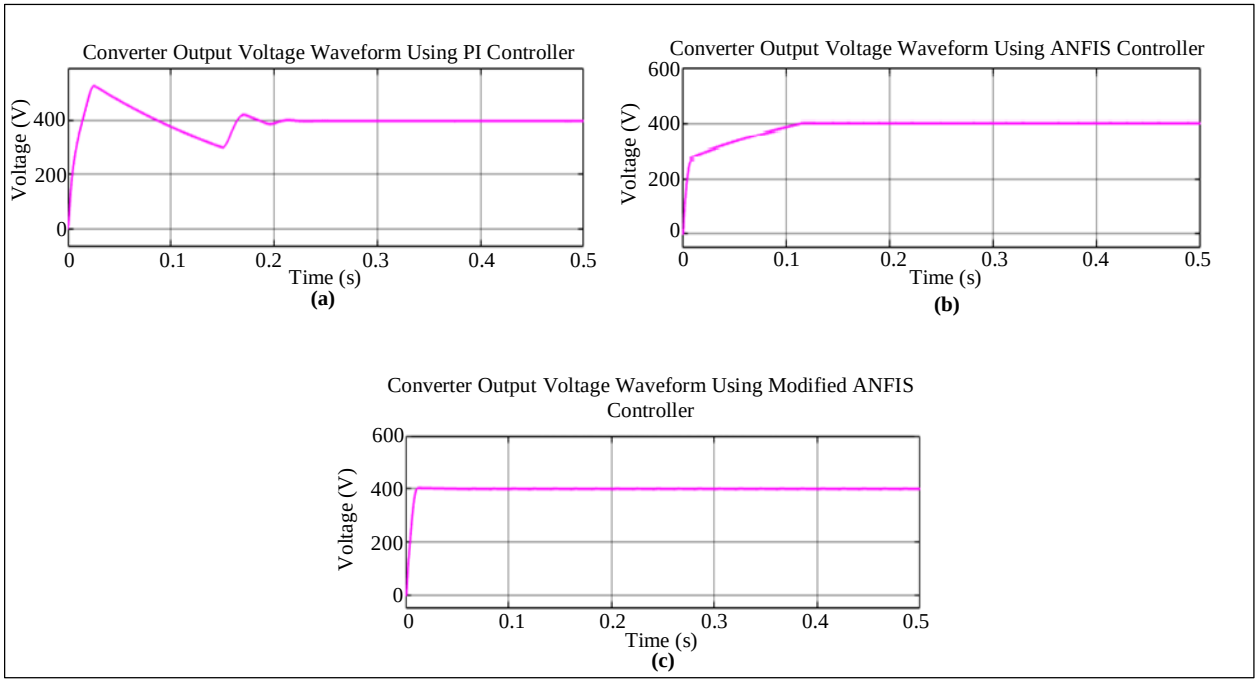

Fig. 16 Converter output voltage waveform using (a) PI controller, (b) ANFIS, and (c) Modified ANFIS controller.

The developed High-gain multi-port converter is contrasted with the conventional techniques, as mentioned in Ref [22-24], to illustrate the prominence of the implemented work. From the comparison graph, it is evident that the proposed framework attained a high-efficiency value of 92% compared to the conventional topologies, as illustrated in Figure 17. Figure 18 specifies the comparison of switching losses, which analyzed that the developed high gain DC-DC converter has reduced switching losses of 9W contrasted to the other conventional techniques.

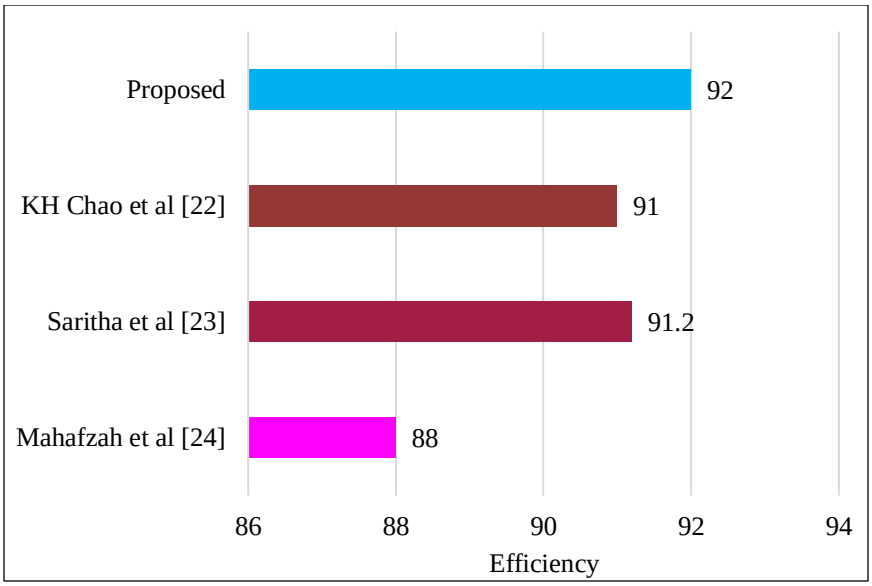

Fig. 17 Comparison of efficiency

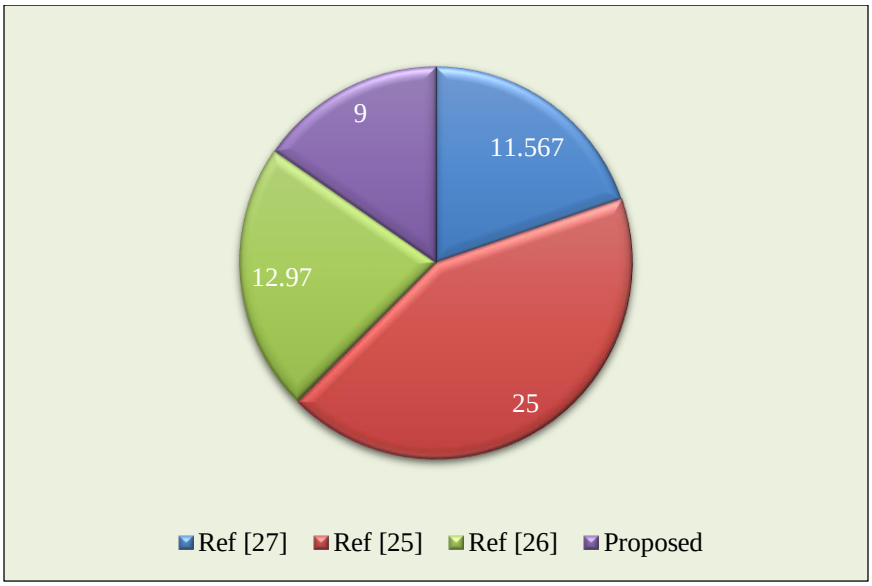

Fig. 18 Comparison of switching losses

Table 2. Comparison of various controllers

Controllers	Settling Time (s)	Rise Time (s)
PI	0.2	0.01
ANFIS	0.12	0.01
Proposed Modified ANIFS	0.02	0.01

4. Conclusion

In this paper, a high-gain multi-port DC-DC converter and modified ANFIS control are proposed for a robust DC power supply. The developed converter efficiently manages the power flow between multiple sources and loads. It allows for the effective integration of various energy sources, such as PV arrays, batteries and the load, while ensuring optimal power transfer and system performance. The modified ANFIS control algorithm enhances the robustness and stability of the DC power supply. By continuously monitoring and adjusting the control parameters, ANFIS adapt to varying environmental conditions and load demands, ensuring a

reliable and efficient power supply. Moreover, the battery system effectively stores the surplus energy and distributes it to the load during the lagging period of energy from the PV system. The overall developed system is executed in MATLAB/Simulink, and it is contrasted with the conventional topologies to show the prominence of the developed work. The results demonstrate that by utilizing the developed converter and control technique, the higher efficiency of 92%, reduced switching loss of 9W and settling time of 0.02 is attained.

References

[1] T.V.V. Pavan Kumar et al., "A Highly Consistent and Proficient Class of Multiport DC-DC Converter Based Sustainable Energy Sources," *Materials Today: Proceedings*, vol. 56, pp. 1758-1768, 2022. [CrossRef] [Google Scholar] [Publisher Link]

[2] Ali M. Jasim et al., "A Novel Cooperative Control Technique for Hybrid AC/DC Smart Microgrid Converters," *IEEE Access*, vol. 11, pp. 2164-2181, 2023. [CrossRef] [Google Scholar] [Publisher Link]

[3] Nagwa F. Ibrahim et al., "Multiport Converter Utility Interface with a High-Frequency Link for Interfacing Clean Energy Sources (PV\Wind\Fuel Cell) and Battery to the Power System: Application of the HHA Algorithm," *Sustainability*, vol. 15, no. 18, pp. 1-25, 2023. [CrossRef] [Google Scholar] [Publisher Link]

[4] Md. Abdullah-Al-Mahbub et al., "Different Forms of Solar Energy Progress: The Fast-Growing Eco-Friendly Energy Source in Bangladesh for a Sustainable Future," *Energies*, vol. 15, no. 18, pp. 1-28, 2022. [CrossRef] [Google Scholar] [Publisher Link]

[5] Md. Sanwar Hossain et al., "Solar PV and Biomass Resources-Based Sustainable Energy Supply for Off-Grid Cellular Base Stations," *IEEE Access*, vol. 8, pp. 53817-53840, 2020. [CrossRef] [Google Scholar] [Publisher Link]

[6] Johny Renoald Albert, "Design and Investigation of Solar PV Fed Single-Source Voltage-Lift Multilevel Inverter Using Intelligent Controllers," *Journal of Control, Automation and Electrical Systems*, vol. 33, no. 5, pp. 1537-1562, 2022. [CrossRef] [Google Scholar] [Publisher Link]

[7] Vaibhav Uttam Pawaskar, Ghanshyamsinh Gohil, and Poras T. Balsara, "Study of Voltage Balancing Techniques for Series-Connected Insulated Gate Power Devices," *IEEE Journal of Emerging and Selected Topics in Power Electronics*, vol. 10, no. 2, pp. 2380-2394, 2022. [CrossRef] [Google Scholar] [Publisher Link]

[8] Chi K. Tse et al., "Circuits and Systems Issues in Power Electronics Penetrated Power Grid," *IEEE Open Journal of Circuits and Systems*, vol. 1, pp. 140-156, 2020. [CrossRef] [Google Scholar] [Publisher Link]

[9] Kashmala Salim et al., "Low-Stress and Optimum Design of Boost Converter for Renewable Energy Systems," *Micromachines*, vol. 13, no. 7, pp. 1-22, 2022. [CrossRef] [Google Scholar] [Publisher Link]

[10] Mamdouh L. Alghaythi et al., "A High Step-Up Interleaved DC-DC Converter with Voltage Multiplier and Coupled Inductors for Renewable Energy Systems," *IEEE Access*, vol. 8, pp. 123165-123174, 2020. [CrossRef] [Google Scholar] [Publisher Link]

[11] Zhaoyang Zhao et al., "Online Capacitance Monitoring for DC/DC Boost Converters Based on Low-Sampling-Rate Approach," *IEEE Journal of Emerging and Selected Topics in Power Electronics*, vol. 10, no. 5, pp. 5192-5204, 2021. [CrossRef] [Google Scholar] [Publisher Link]

[12] Zhen Pan et al., "Enhancement of Maximum Power Point Tracking Technique Based on PV-Battery System Using Hybrid BAT Algorithm and Fuzzy Controller," *Journal of Cleaner Production*, vol. 274, 2020. [CrossRef] [Google Scholar] [Publisher Link]

[13] Mohammed Ali Khan et al., "Advanced Control Strategy with Voltage Sag Classification for Single-Phase Grid-Connected Photovoltaic System," *IEEE Journal of Emerging and Selected Topics in Industrial Electronics*, vol. 3, no. 2, pp. 258-269, 2022. [CrossRef] [Google Scholar] [Publisher Link]

[14] A. Senthilnathan et al., "Fuzzy Logic Controlled 3 Port DC to DC Cuk Converter with IoT Based PV Panel Monitoring System," *International Journal of System Assurance Engineering and Management*, pp. 1-9, 2022. [CrossRef] [Google Scholar] [Publisher Link]

[15] Lotfi Farah et al., "A Highly-Efficient Fuzzy-Based Controller with High Reduction Inputs and Membership Functions for a Grid-Connected Photovoltaic System," *IEEE Access*, vol. 8, pp. 163225-163237, 2020. [CrossRef] [Google Scholar] [Publisher Link]

[16] Daming Wang et al., "Model Predictive Control Using Artificial Neural Network for Power Converters," *IEEE Transactions on Industrial Electronics*, vol. 69, no. 4, pp. 3689-3699, 2022. [CrossRef] [Google Scholar] [Publisher Link]

[17] Md. Ariful Islam et al., "Modeling and Performance Evaluation of ANFIS Controller-Based Bidirectional Power Management Scheme in Plug-in Electric Vehicles Integrated with Electric Grid," *IEEE Access*, vol. 9, pp. 166762-166780, 2021. [CrossRef] [Google Scholar] [Publisher Link]

[18] Hesham M. Fekry et al., "Power Management Strategy Based on Adaptive Neuro Fuzzy Inference System for AC Microgrid," *IEEE Access*, vol. 8, pp. 192087-192100, 2020. [CrossRef] [Google Scholar] [Publisher Link]

[19] Majid Mehrasa et al., "Passivity ANFIS-Based Control for an Intelligent Compact Multilevel Converter," *IEEE Transactions on Industrial Informatics*, vol. 17, no. 8, pp. 5141-5151, 2021. [CrossRef] [Google Scholar] [Publisher Link]

[20] Mahmoud Elsisi et al., "Robust Design of ANFIS-Based Blade Pitch Controller for Wind Energy Conversion Systems against Wind Speed Fluctuations," *IEEE Access*, vol. 9, pp. 37894-37904, 2021. [CrossRef] [Google Scholar] [Publisher Link]

[21] Metehan Guzel et al., "ANFIS and Deep Learning Based Missing Sensor Data Prediction in IoT," *Concurrency and Computation: Practice and Experience*, vol. 32, no. 2, 2020. [CrossRef] [Google Scholar] [Publisher Link]

[22] Kuei-Hsiang Chao, Ying-Piao Kuo, and Hong-Han Chen, "Design and Implementation of a Soft-Switching Converter with High Step-Up Ratio," *IEEE Access*, vol. 11, pp. 48506-48516, 2023. [CrossRef] [Google Scholar] [Publisher Link]

[23] P. Saritha et al., "Design and Analysis of Multiple Input Single Output Converter for Hybrid Renewable Energy System with Energy Storage Capability," *Ain Shams Engineering Journal*, vol. 14, no. 10, 2023. [CrossRef] [Google Scholar] [Publisher Link]

[24] Khaled A. Mahafzah et al., "A New Cuk-Based DC-DC Converter with Improved Efficiency and Lower Rated Voltage of Coupling Capacitor," *Sustainability*, vol. 15, no. 11, pp. 1-17, 2023. [CrossRef] [Google Scholar] [Publisher Link]

[25] Farha Khan et al., "A New Non-Isolated High-Gain DC-DC Converter for the PV Application," *e-Prime-Advances in Electrical Engineering, Electronics and Energy*, vol. 5, pp. 1-20, 2023. [CrossRef] [Google Scholar] [Publisher Link]

[26] Mahajan Sagar Bhaskar et al., "A New Triple-Switch-Triple-Mode High Step-Up Converter with Wide Range of Duty Cycle for DC Microgrid Applications," *IEEE Transactions on Industry Applications*, vol. 55, no. 6, pp. 7425-7441, 2019. [CrossRef] [Google Scholar] [Publisher Link]

[27] Chih-Lung Shen et al., "Multi-Port Multi-Directional Converter with Multi-Mode Operation and Leakage Energy Recycling for Green Energy Processing," *Energies*, vol. 15, no. 15, pp. 1-26, 2022. [CrossRef] [Google Scholar] [Publisher Link]